Mathematical Methods in the Applied Sciences

Detecting 3D multistability with a meshfree reconstruction of invariant manifolds of saddle point

Journal:	*Mathematical Methods in the Applied Sciences*
Manuscript ID	Draft
Wiley - Manuscript type:	Special Issue Paper
Date Submitted by the Author:	n/a
Complete List of Authors:	Francomano, Elisa; University of Palermo, Department of Industrial and Digital Innovation, Numerical Section Paliaga, Marta; University of Palermo, Department of Industrial and Digital Innovation, Numerical Section
Keyword:	Dynamical systems, Separatrix, saddle points, invariant manifold, meshfree method, Moving Least Squares

Received ; | Revised ; | Accepted
DOI: xxx/xxxx

RESEARCH ARTICLE

Detecting 3D multistability with a meshfree reconstruction of invariant manifolds of saddle point

Elisa Francomano* | Marta Paliaga

[1]Scuola Politecnica, DIID, University of Palermo, Italy

Correspondence
*Elisa Francomano, Email: elisa.francomano@unipa.it

Abstract

In mathematical modeling, it is often required the analysis of the vector field topology in order to predict the evolutions of the variables involved. When the dynamical system shows a multi-stability the trajectories have different configuration depending on the initial conditions.
The aim of this work is the analysis of the boundaries of the different basins of attraction by means the detection of the invariant manifolds of the saddle points. We show as the detection method works with different number of stable points and in presence of strange attractors. Once that a sufficient number of separatrix points is found, a Moving Least Squares meshfree method is involved for the reconstruction. Numerical results are presented to assess the method.

KEYWORDS:
Dynamical systems, separatrix, saddle points, invariant manifold, meshfree method, Moving Least Squares

1 | INTRODUCTION

Mathematical modeling and experimental investigations are nowadays commonly used in applied sciences to explain biological or physics process[4,11,30]. The dynamics within the phenomenon studied can be modeled by means of unknown and suitable parameters to describe their interactions.
One of the most important goal is the analysis of the vector field topology, i.e. the space of all solutions, in order to predict the possible outcomes of the system. The trajectories, or solutions, are completely determined by the parameters value and the different initial conditions. In fact, changing the set of parameters usually leads to the appearance (or disappearance) of alternative stable states[27,11,32]. While, when a dynamical system admits more than one steady state, the phase-space is thus partitioned into different regions, called basins of attraction. In this case the final configuration of a process depends on the domain to which the initial condition belongs.
The aim of this work is the reconstruction of the boundaries of these basins to have a completely knowledge of the vector field dynamics. This approach allows to modify or to avoid the initial state too close to the boundaries that are subject to shift from one basin to another. These regime shifts are very common in the biological process and they can lead to undesirable configuration of the model such as the extinction of a specie[9], collapse of fisheries[31] or the destruction of the coral reef[29].

The simpler way to visualize the domains of the phase space is the graphical representation of the separatrix surfaces, therefore the main goal is to develop an algorithm that could be easy used by the biologist, the ecologist or the medical researchers that are investigating on the dynamical process. The first attempt in graphical representation of these surfaces is presented in[12–15].

The authors developed a bisection method to detect the separatrix points coupled with a Partition of Unity meshfree method to reconstructed them. Following these ideas in [19], [20], [21], we give a complete analysis of the Allee effect induced by the pack hunting in a predator-prey model [25]. We reconstruct the separatrix with a Moving Least Squares method to avoid the resolution of the interpolation system. In particular we adapted the bisection method to the model considered in order to reduce the computational effort. However it still remains quite expensive, therefore we oriented the research to the topological features of the critical points. Although in vector field analysis the algorithms are well formulated in 2D systems [8], [24], [28], [36], only little attempts exist to analyze the 3D models [22], [34], [35]. We extend these results, obtaining a new numerical approach to detect the points of the separatrix surfaces by considering the stable and the unstable manifolds of the saddle points. Indeed they divide the phase domain into invariant flow regions, representing themselves the boundaries of the attractor domain.
Here we show as the algorithm developed works for the three dimensional multi-stable models with any number of steady states simultaneously stable. Usually an attractor is represented by a fixed point, however persistent oscillation or chaotic behavior could arise. We demonstrate that the reconstruction of the separatrix is possible even in presence of these strange attractors. The article is organized as follow. In Section 2 we present the main topic in vector field topology introducing the notation used in the other sections. Then we describe the two different phases of the algorithm developed in Section 3 and 4. To test our method we present two different case studies in Section 5. Finally some conclusions are given.

2 | CRITICAL POINTS TOPOLOGY IN 3D MODELS

Given a three dimensional vector field: $\dot{u} = F(u)$ with $u : E^3 \to \mathbb{R}^3$ and F a linear or non linear functional, a first order critical point x_0 is a fixed point ($\dot{u}(x_0) = 0$), such that $J(x_0) \neq 0$, where J is the Jacobian matrix associated to the system [30]. Through the analysis of the eigenvalues of $J(x_0)$ it is possible classified the critical points as follow:

Stable Point	$\mathrm{Re}(\lambda_1) < \mathrm{Re}(\lambda_2) < \mathrm{Re}(\lambda_3) < 0$
Unstable Point	$0 < \mathrm{Re}(\lambda_1) < \mathrm{Re}(\lambda_2) < \mathrm{Re}(\lambda_3)$
Repelling Saddle	$\mathrm{Re}(\lambda_1) < 0 < \mathrm{Re}(\lambda_2) < \mathrm{Re}(\lambda_3)$
Attracting Saddle	$\mathrm{Re}(\lambda_1) < \mathrm{Re}(\lambda_2) < 0 < \mathrm{Re}(\lambda_3)$

where $Re(\lambda_i)_{i=1,2,3}$ represents the real part of the three eigenvalues $\lambda_1, \lambda_2, \lambda_3$.
This general classification is divided into other subclasses depending on the nature of the eigenvalues. Indeed when the Jacobian admits two conjugate complex eigenvalues the points are called "focus".
In a neighborood of the stable points all the trajectories converge to the point itself. In this case all the eigenvalues are independent. When the stable point is a focus the only real eigenvalue describes the direction of the straight inflow, in addiction the plane generated by the two complex eigenvectors contain all the trajectories tending to the critical point but they spiral around it. Inverse behavior is observed for the unstable point for which all the trajectories diverge from it.
The saddles are always unstable steady state because at least one eigenvalues has a positive real part. However an attracting saddle has one direction of outflow behavior and a plane in which all the stream lines collapse to the point. Opposite behavior works for the repelling saddle.
The separatrix surfaces that we are looking for are manifold that partitioned the phase-space into basins with different flow behavior. Since around the stable/unstable points the trajectories are homogenous, these particular steady state are not involved on the reconstruction of the surfaces. On the contrary the saddle points possess two different kind of invariant manifold that represents the separatrices themselves.
If $\mathbf{x}_0 \in \mathbb{R}^3$ is a saddle, the stable manifold $W^s(\mathbf{x}_s)$ has the property that all its orbits tend to the saddle in forward time:

$$W^s(\mathbf{x}_s) = \left\{\mathbf{x} \in E^3 \,|\, \lim_{t\to+\infty} u(\mathbf{x}, t) = \mathbf{x}_0\right\}.$$

On the other hand, the unstable manifold $W^u(\mathbf{x}_s)$ is generated by the eigenvalues with positive real part, and it includes all the trajectories tending to $\mathbf{x}_s$ in backward time:

$$W^u(\mathbf{x}_s) = \left\{\mathbf{x} \in E^3 \,|\, \lim_{t\to-\infty} u(\mathbf{x}, t) = \mathbf{x}_0\right\}.$$

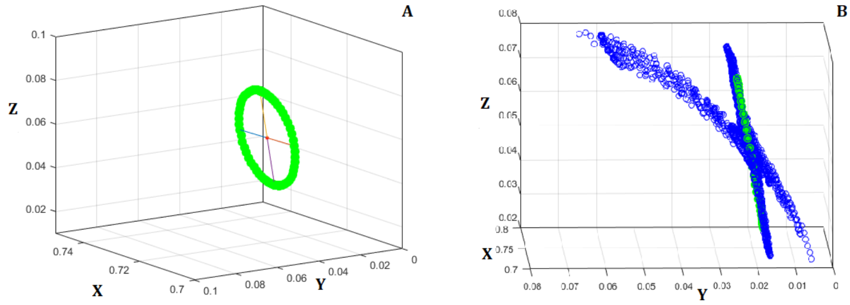

FIGURE 1 A) Seeding points on the ellipse generated by the two eigenvectors v_1 and v_2. B) Integration of the trajectories starting from the seeding points.

3 | INVARIANT MANIFOLD RECONSTRUCTION

In the following we illustrate the basic idea used to approximate the invariant manifolds of saddle points.
We describe the computational approaches adopted to find a sufficient number of scattered data on the separatrix surfaces or curves.
The analysis considers only the three dimensional models, however the same procedure can be applied to the linear or bi-dimensional model.

3.1 | Detection of the separatrix points

In previous section we have presented the most important characteristic of the vector field and its possible critical points. In particular we have highlighted about the invariant manifolds of the saddle. In this paragraph we present the first part of the algorithm dedicated to the detection of the manifold scattered data.
The general idea is finding the bidimensional manifold for each saddle $x_s \in \mathbb{R}^3$. The first step is calculate and analyze the Jacobian matrix $J(x_s)$ by finding the respective eigenvalues λ_i and eigenvectors v_i with $i = 1, 2, 3$ (Step 1).
If the saddle is repelling there are two eigenvalues with positive real part. Therefore the corresponding eigenvectors generate a plane E^u that is tangent to the unstable manifold W^u [23]. While if the saddle is attracting the eigenvectors v_1 and v_2 generate a plane E^s that is tangent to the stable manifold W^s.
Different procedure is applied if there is a saddle-focus because the two eigenvectors generating the subspace $E^{s(u)}$ are complex conjugated such that :

$$Re(v1) = Re(v2) \text{ and } Im(v1) = -Im(v2).$$

Therefore, in this case we consider as first generating vector the real part and as second the imaginary part (Step 2.1).
Now, to integrate the points on the invariant manifold we place N points on an ellipse centered at the saddle whose semi-axes are the corresponding eigenvectors (Figure 1 A). They serve as seeding points of the separatrix surface. Because these points belong to the invariant manifold all their trajectories lye on the manifold itself. Therefore we numerical integrate the seeding points flow. We use a fourth order Runge-Kutta method and the direction of the integration depends on the topology of the saddle considered: forward in time for repelling saddle and backward in time for the attracting one (Step 4).
To reconstruct the separatrix is necessary identify the scattered data, thus for each trajectory we identify the state obtained for each step of integration (Figure 1 B). When the system has more than two stable attractors as consequence we have more than one saddle point. In this case we have to reconstruct more separatrix manifold by applying the same procedure for each one (Step 5). Similar procedure is applied to find the one dimensional curve W^u. In this case we integrate the flow starting from a point of the unstable eigenvectors v_3.

In the following we report the sketch of the computational process developed:

- - **s** $\in \mathbb{R}^{nx3}$: is a matrix whose rows contain the saddle of the model.
- - **parameter** $\in \mathbb{R}^{1xk}$: the parameters vector.
- - **l** $\in \mathbb{R}$: the edge length of the cubic domain considered.
- - **t** $\in \mathbb{R}$: size of integration interval.
- - **M** $\in \mathbb{R}$: number of the seeding points on the ellipse.
- - ***String***: A string with the name of the 3D model that it is considered.

- **STEP 1** Consider one saddle point $x_s \in E$ and calculate the Jacobian matrix $J(x_s)$.
- **STEP 2** Calculate and order the eigenvectors and eigenvalues in ascending order:
  $V = [v_1; v_2; v_3]$ such that $Re(\lambda_1) < Re(\lambda_2) < Re(\lambda_3)$
  STEP 2.1 ***if*** v_1 and v_2 are complex conjugated
  $$\textbf{\textit{then}}\ v_1 = Re(v_1) \wedge v_2 = Im(v_1)$$
- **STEP 3** ***for*** $i = 0 : M$
  STEP 3.1 Consider the i-th point on the ellipse:
  $$x = i * pi/M;\ y = (1 - cos(x))/2 * pi;$$
  $$v = cos(x) * v2 + sin(y) * v_1;$$
  STEP 3.2 Define the initial condition : $z = x_s + v$.
  STEP 3.3 Integrate the system in the interval $[0, t]$.
  $$\textbf{\textit{if}}\ \lambda_1 < 0 \wedge \lambda_2 < 0\ \textbf{\textit{then}}\ t = -t$$
  $$[t, u] = ode45(@system, [0, t], parameter, z)$$
- **STEP 4** Plot the scattered data on the phase-plane:
  scatter3(u(:,1),u(:,2),u(:,3));
- **STEP 5** Repeat the procedure for each saddle point.

---

4 | MOVING LEAST SQUARES METHOD

Given a set of data, i.e measurements obtained from the experimental investigation, the aim of the numerical algorithm is to find a function **G** that is a good fit for these data. As we observed in Figure 1 A the scattered data are not always gridded or uniform distributed therefore it is necessary impose some conditions to the approximant ***G*** to obtain a satisfy result.
In this section we present a Moving Least Square method that achieve a polynomial reproduction approximation of any order d. In particular we use a mesh-free approach that allows to work with a large number of data and that it is not influenced by the geometry domain[1–3,10,18].
In our case the set of data are the M scattered points of the separatrix manifold projected on the plane XY obtaining the set

$\chi = \{\mathbf{x}_1, ..., \mathbf{x}_M\} \subset \mathbb{R}^2$ and the heights $\{z_i | i = 1, ..., M\}$ represents the set of the data values.
The general idea of the MLS is to calculate the generating functions $\Phi_i(\mathbf{y}) = \Phi(\mathbf{y}, \mathbf{x}_i)$ necessary for the construction of the quasi-interpolant[5]:

$$G(\mathbf{y}) = \sum_{i=1}^{M} f(\mathbf{x}_i)\Phi_i(\mathbf{y}). \tag{1}$$

First, to achieve a certain order of approximation, the generating functions have to minimize the least-squares quantity:

$$\frac{1}{2}\sum_{i=1}^{M} \Phi_i^2(\mathbf{y})\frac{1}{\omega(\mathbf{x}_i, \mathbf{y})}, \tag{2}$$

that depends on the weight functions ω that govern the influence of data x_i in the approximation of the evaluation point $\mathbf{y}$.
Usually the radial basis functions represent a good choice, because they depend only on the distance between the two arguments: $r = ||x_i - y||_2$ and becomes smaller the further away from each other its arguments are.
Specifically we use the Wendland C2 supported compacted centered on $\mathbf{y}$:

$$\omega(\mathbf{x}_i, \mathbf{y}) = (1 - \epsilon||\mathbf{y} - \mathbf{x}_i||_2)_+^4(4\epsilon||\mathbf{y} - \mathbf{x}_i||_2 + 1). \tag{3}$$

Therefore, in the construction of the approximant, the data values x_i outside the support are not considered, reducing the computational cost.
Let $Q = span\{p_1, ..., p_m\}$ with $m < N$ the approximation space with $p_m \in \prod_2^d$, the space of the bi-variate polynomial of degree at most d, imposing the polynomial constraints:

$$\sum_{i=1}^{M} p(\mathbf{x}_i)\Phi_i(\mathbf{y}) = p(\mathbf{y}) \quad \forall p \in \mathbf{\Pi}_2^d, \tag{4}$$

we ensure that the quasi-interpolant P reproduces polynomials of a certain degree d. The generating functions Φ satisfying (2) and (4) are given by[37]:

$$\Phi_i(\mathbf{y}) = \omega(\mathbf{x}_i, \mathbf{y})\sum_{j=1}^{m} \lambda_j p_j(\mathbf{x}_i), \quad i = 1, ...M \tag{5}$$

where λ_k are the Lagrange multipliers, i.e. the only solutions of the Gram system:

$$\sum_{i=1}^{M} p_k(\mathbf{x}_i)p_l(\mathbf{x}_i)\omega(\mathbf{x}_i, \mathbf{y})\lambda(\mathbf{y}) = p(\mathbf{y})\; k, l = 1, ..., m. \tag{6}$$

In our case, by imposing a linear reproduction, the Gram systems are three dimensional, thus we find the explicit formula for the multipliers by avoiding to solve any system[17].
The computational cost for each evaluation point y is reduced and it is limited by the quantity:

$$O(Q^3 + Q^2 I_y + Q I_y), \tag{7}$$

where I_y is the number of the data values x_i lying on the support of the weighted function centered on y.

5 | NUMERICAL EXAMPLES

In this section we reconstruct the separatrix for two eco-epidemiological model, in order to test the algorithm. In the first example, the system analyzed has three stable state, therefore we reconstruct the invariant manifold of the two different saddle nodes. In the second one, we demonstrate that the algorithm works in presence of strange attractors.

5.1 | Tristable predator-prey model

Let consider the following dynamical system[26]:

$$\frac{dS}{dt} = S\left[(S-\theta)(1-S-I) - \beta I - aP\right], \tag{8}$$

$$\frac{dI}{dt} = \beta S I - a I P - \mu I, \tag{9}$$

$$\frac{dP}{dt} = P\left[bs + \alpha I - d\right]. \tag{10}$$

It analyzes a predator-prey interaction with prey subjected to Allee effect and disease. Therefore these latter are divided into *susceptible* (S) and *infected* (I) individuals and P represents the predators density. The model is already in an a-dimensional form where the parameters involved are resumed in the following table:

Parameter	Biological Meaning
θ	Allee threshold
β	Infection Rate
a	Attack rate of predator
b	Total effect to predator by consuming susceptible prey
μ	Death rate of infected prey
α	Total effect to predator by consuming infected prey
d	Natural death rate of predator.

Letting $\beta = 1.5$, $\theta = 0.2$, $a = 2$, $b = 1.35$, $\mu = 1$ and $d = 1$ the system admits three stable equilibria: the origin $E_0 \equiv (0,0,0)$, the disappearance of the disease $E_1 \approx (0.7407, 0, 0.0701)$ and the predator extinction $E_2 \approx (0.6667, 0.0791, 0)$.
For the reconstruction of their basins of attraction we consider the invariant manifolds of the attractive saddle points $E_{s_1} \equiv (\theta, 0, 0)$ and $E_{s_2} \approx (0.7329, 0.0211, 0.0497)$.
We start with the first saddle that admits the stable eigenvectors $v_1 \approx (0.4099, 0, 0.9121)$ and $v_2 \approx (0.329, 0.9442, 0)$. We integrate the separatrix considering $M = 20$ equispaced on the ellipse generated by v_1 and v_2. Then, through a backward integration we obtain all the scattered data on the manifold (Figure 2 A).
Applying the same procedure to the saddle E_{s_2} we generate the separatrix points on the second manifold taking the stable complex conjugated eigenvectors $v_{1,2} \approx (0.9817, -0.0088 \pm 0.08731i, -0.0552 \pm 0.1599i)$. (Figure 2 B).
Finally we approximate the two surfaces (Figure 2 C) applying the MLS approximant using the Wendland C2 compactly supported function:

$$\omega(\mathbf{x}_i, \mathbf{y}) = (1 - \epsilon||\mathbf{y} - \mathbf{x}_i||_2)_+^4 (4\epsilon||\mathbf{y} - \mathbf{x}_i||_2 + 1) \tag{11}$$

where the *shape parameter* $\epsilon = 3$ and 60 evaluation points $\mathbf{y}$ are taking into account (Figure 2 D).

5.2 | Separatrix manifold and strange attractor

Now, we present another predator-prey model but this time we consider a set of parameters value that induce a complex dynamics with the appearance of strange attractor. Usually an attractor is a fixed stable point, however in eco-epidemiological modeling is very common the presence of persistent oscillation after particular bifurcation point.
In[7] the authors analyze two relatively eco-epidemiological models, but we present only the study of the system with density dependent transmission[6]:

$$\frac{dS}{dt} = rN(1-N) - \frac{NP}{h+N}, \tag{12}$$

$$\frac{dI}{dt} = \frac{NP}{h+N} - mP - \mu I P, \tag{13}$$

$$\frac{dP}{dt} = i\left((\beta - \mu)(1-i) - \frac{NP}{h+N}\right). \tag{14}$$

This represents the a-dimensional form. N is the prey density that grows logistically in absence of the predator population with a per capita growth rate r. They decrease because of the predation modeled by an Holling Type II functional response ($\frac{NP}{h+N}$).
The predators P are infected by an SI disease, therefore there is no recovery and it is not considered a vertical transmission, from mothers to the newborns. To analyze the effect of the disease in the predator-prey dynamics, the authors replace the densities of susceptible *(S)* and infected *(I)* with the entire population P and the prevalence of the disease i, i.e. the fraction of the infected

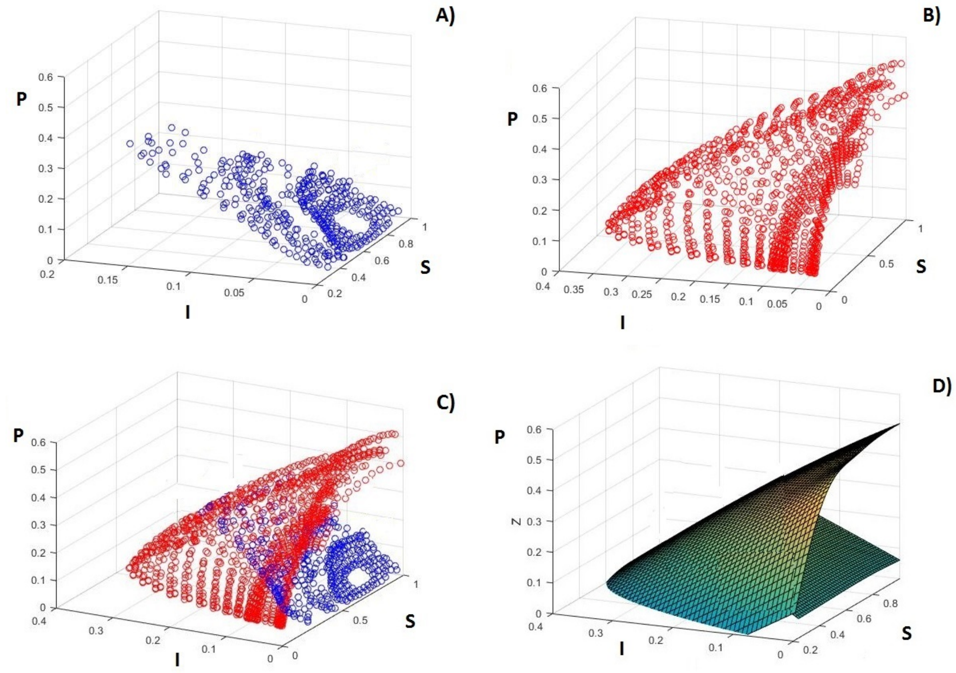

FIGURE 2 A) Scattered data on invariant manifold of saddle E_{s_1}; B) Scattered data on invariant manifold of saddle E_{s_2}; C) Intersection of the two separatricies; D) Reconstruction of the two surfaces.

on the entire predator density: $i = I/P$.
The predators decrease because the per capita death-rate m and the infected suffer of an additional mortality μ disease-induced. Finally β represents the transmissibility.
Despite the simplicity of the model the authors observe quasi-periodicity, torus, oscillation and even chaos. Such complex behavior means that small changes to parameters or initial conditions can have large effect on the biological system in long term. Therefore the reconstruction of the separatrix offers an important tool to study the vector field and the biological dynamics.
When $\mu = 2, r = 0.5, h = 0.1, m = 0.2, \beta = 27$ the system is tri-stable between the disease-free predator prey oscillation, a coexistent torus and the coexistent equilibrium $E_1 \approx\equiv (0.6884, 0.1228, 0.366)$.
Here we reconstruct the separatrix manifold between the oscillation and the steady state E_1 by considering the other coexistence point $E_2 \approx (0.1282, 0.995, 0.5)$.
The Jacobian matrix admits two complex conjugate eigenvalues λ_1 and λ_2 and one real positive λ_3, presenting an attractive saddle.
We take $N = 20$ points on the ellipse generated by the two vectors: $v_1 \approx (0.1294, -0.0129, -0.9638)$ and $v_2 \approx (-0.0358, -0.228, 0)$, representing respectively, the real and the imaginary part of the complex eigenvectors. In Figure 3 A the red curve evolves toward the fixed point while the green one oscillate.
Finally the manifold is reconstructed by considering again the Wendland C2 function with the shape parameter $\epsilon = 2$ (Figure 3 B)

6 | CONCLUSIONS

In this paper we present a new strategy to detect the invariant manifold of the saddle points. These surfaces are fundamental to the dynamical analysis of multi-stable models because they partitioned the phase-space into disjoint regions of different flow behavior.
Furthermore, by representing these surfaces, it is possible predict the possible evolution for each initial conditions.
We show that the algorithm presented works for every 3D models with a different number of equilibrium points contemporary

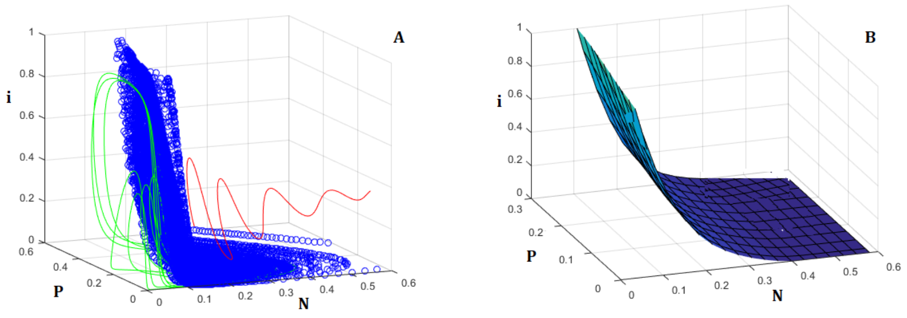

FIGURE 3 A)In blu the scattered data lying on the invariant manifold. In red it is represented the trajectory of the point $P_1 \equiv (0.2, 0.2, 0.2)$, in green the trajectory of the point $P_2 \equiv (0.1, 0.2, 0.4)$ evolves toward the coexistent thorus. The values of the parameters are: $\mu = 2, r = 0.5, h = 0.1, m = 0.2, \beta = 27$. B) Reconstruction of the surface

stale. In fact the detection of the manifold depends only on the saddle node.
We extend the previous results showing that, even in presence of strange attractors, such as torus or limit cycle, the algorithm still works. This kind of detection strategies yields good results for most topologies except for focus saddle with strong circulation that can intersect the seeding ellipse. Future work is devoted on solving these problems, by opportunely involving the bisection method coupled with our strategy.

ACKNOWLEDGEMENTS

The research has been supported by the Istituto Nazionale di Alta Matematica - INDAM - GNCS Project 2017 and it has been accomplished within the RITA "Research ITalian network on Approximation".

BIBLIOGRAPHY

References

1. G. Ala, G.E. Fasshauer, E. Francomano, S. Ganci and M.J. McCourt, A meshfree solver for the MEG forward problem, IEEE Transactions on Magnetics, Vol. 51(3), 5000304 (2015).
2. G. Ala, G.E. Fasshauer, E. Francomano, S. Ganci and M.J. McCourt, An augumented MFS approach for brain activity reconstruction, Mathematics and Computers in Simulation, Article in press, DOI 10.1016/j.matcom.2016.11.009 (2016).
3. G. Ala, G.E. Fasshauer, E. Francomano, S. Ganci and M.J. McCourt, The method of Fundamental Solutions in solving coupled boundary value problems for M/EEG, SIAM, Journal on Scientific Computing, Vol. 37(4), B570-B590 (2015).
4. W.C. Allee, Animal Aggregations. A study in General Sociology. University of Chicago Press, Chicago (1931).
5. G. Backus and F. Gilbert, The resolving power of gross earth data, Geophys. J. R. Astr. Soc., Vol. 16, 169–205 (1968).
6. A.M. Bate and F.M. Hilker, Disease in group-defending prey can benefit predators, Theoretical Ecology, Vol. 7, 87–10 (2014).
7. A.M. Bate and F.M. Hilker, Complex Dynamics in an Eco-epidemiological Model, Bull. Math. Biol., Vol. 75, 2059–2078 (2013)
8. R. Batra and L. Hesselink, Topology based vector field comparison using graph methods, In Proceeding IEEE Visualization '99, 25–28 (1999).
9. D.D. Briske, S.D. Fuhlendorf and F.E. Smeins, A unified framework for assessment and application of ecological thresholds, Rangeland Ecology & Management, Vol. 59, 225–236 (2006).

10. M.D. Buhmann, S. De Marchi and G. Plonka-Hoch, Kernel Functions and Meshless Methods, Dolomites Research Notes on Approximation, 4 (Special Issue), 1–63 (2011).

11. S.R. Carpenter, D. Ludwig and W.A. Brock, Management of eutrophication for lakes subject to potentially irreversible change, Ecological Applications, Vol. 9, 751–771 (1999).

12. R. Cavoretto, S. De Marchi, A. De Rossi, E. Perracchione and G. Santin, Approximating basins of attraction for dynamical systems via stable radial bases, AIP Conference Proceedings, Vol. 1738, 390003-1–390003-4 (2016).

13. R. Cavoretto, A. De Rossi, E. Perracchione and E. Venturino, Graphical Representation of separatrices of attraction basins in two and three-dimensional dynamical systems, International Journal of Computational Methods, Vol. 14, 1750008-1–1750008-16 (2017).

14. R. Cavoretto, A. De Rossi, E. Perracchione and E. Venturino, Robust approximation algorithms for the detection of attraction basins in dynamical systems, Journal of Scientific Computing, Vol. 68, 395–415 (2016).

15. R. Cavoretto, A. De Rossi, E. Perracchione and E. Venturino, Reliable approximation of separatrix manifolds in competition models with safety niches, International Journal of Computer Mathematics, Vol. 92, 1826–1837 (2015).

16. F. Courchamp, L. Berec and J. Gascoigne, Allee Effects in Ecology and Conservation. Oxford University Press, New York (2008).

17. G.E. Fassahuer, Meshfree Approximation Methods with MATLAB, World Scientific Publishing Co., Singapore (2007).

18. G.E. Fasshauer, E. Francomano, S. Ganci and M.J. McCourt, A meshfree solver for the MEG forward problem, IEEE Transactions on Magnetics, Vol. 51, Issue 3, 5000304 (2015).

19. E. Francomano, F.M. Hilker, M. Paliaga and E. Venturino, An efficient method to reconstruct invariant manifolds of saddle points, Dolomites Research Notes on Approximation, Vol.10, 25–30 (2017).

20. E. Francomano, F.M. Hilker, M.Paliaga and E. Venturino, On Basins of Attraction for a Predator-Prey Model Via Meshless Approximation, AIP Conference Proceedings, Vol. 1776, 070007-1–07007-4 (2016).

21. E. Francomano, F.M. Hilker, M.Paliaga and E. Venturino, Separatrix reconstruction to identify tipping points in an eco-epidemiological model, Applied Mathematics and Computation, DOI doi.org/10.1016/j.amc.2017.07.022 (2017).

22. A. Globus, C. Levitt and T. Lasinski, A tool for visualizing of three dimensional vector field, Proceedings or the 2nd Conference on Visualization 1991, 33–40 (1991).

23. J. Guckenheimer and P.J. Holmes, Nonlinear Oscillations, Dynamical Systems, and Bifurcations of Vector Fields, Applied Mathematical Sciences, Vol. 42, Berlin, New York: Springer-Verlag (1997).

24. J. Helman and L. Hesselink, Visualizing vector field topology in fluid flows, IEEE Computer Graphics and Applications 11 (May), 36–46 (1991).

25. F.M. Hilker, M. Paliaga and E. Venturino, Diseased Social Predators, Bull. Math. Biol., Vol. 79, Issue 10, 2175-2196 (2017).

26. Y. Kang, S.K. Sasmal, A.R. Bhowmick and J. Chattopadhyay, Dynamics of a predator-prey system with prey subject to Allee effects and disease, Mathematical Biosciences and Engineering, Vol. 11, Issue 4, 877–918 (2014).

27. R.M. May, Thresholds and breakpoints in ecosystems with a multiplicity of stable states, Nature, Vol. 269, 471–477 (1977).

28. G. Moore, Laguerre approximation of stable manifolds with application to connecting orbits, Mathematics and Computation, Vol. 73, 211–242 (2003).

29. P.J. Mumby, A. Hastings and H.J. Edwards, Thresholds and the resilience of Caribbean coral reefs, Nature, Vol. 450, 98–101 (2007).

30. J.D. Murray, Mathematical Biology I: An Introduction, third edition. Springer, New York (2002).

31. R.M. Peterman, A simple mechanism that causes collapsing stability regions in exploited salmonid populations, Journal of Fisheries Research Board of Canada, Vol. 34, 1130–1142 (1977).

32. P. Petraitis, Multiple Stable States in Natural Ecosystems. Oxford University Press, Oxford (2013).

33. J.P. Sutherland, Multiple stable points in natural communities. American Naturalist, Vol. 108, 859–873 (1974).

34. H. Theisel and T. Weinkauf, Vector field metrics based on distance measures of first order critical points, Journal of WSCG, Short communication, Vol. 10, 121–128 (2002).

35. H. Theisel, T. Weinkauf, H.C. Hege and H.P. Seidel, Saddle Connectors- an approach to visualizing the topological skeleton of complex 3D vector fields, Visualization, 2003, IEEE (2003).

36. X. Tricoche, G. Scheuermann, and H. Hagen, A topology simplification method for 2D vector fields. In Proc. IEEE Visualization, 359–366 (2000).

37. H. Wendland, Scattered Data Approximation. Cambridge University Press, Cambridge (2010).

□